Advanced Stereo Matching Algorithm for Three-dimensional Reconstruction of Fracture Surfaces†

Toshio KURODA*, Kenji IKEUCHI** and Yoshihiko KITAGAWA***

Abstract

Stereoscopic scanning electron micrographs were used to reconstruct the microscopic topography of fracture surfaces. By applying an image processing system developed for fractographic analysis, Digital Elevation Models (DEMs) of the investigated surface were obtained using a personal computer. An advanced area-based matching algorithm was developed to reconstruct DEMs from two surface projections. The hierarchical algorithm was applied to the searching procedure, which involved step-by-step decreasing of reference window size to achieve both an increase in the search accuracy and a decrease in the occurrence of matching errors.

At first, the reconstruction procedure was applied by using the conventional area-based algorithm to a Vickers hardness indent, the geometry of which is specified. The result verified the accuracy of the system. For more complicated objects such as the ductile fracture surface of SUS329J3L duplex stainless steel, the advanced hierarchical method was required to obtain an accurate reconstruction. The DEM reconstructed using the advanced stereo matching algorithm revealed the detailed features on the fracture surface such as the shape of the dimple patterns.

KEY WORDS: (Scanning electron microscope) (Fracture surface) (Three-dimension) (Stereo matching) (Image processing) (Fractography)

1. Introduction

Scanning electron microscope (SEM) has been used widely in the field of fractography to obtain information about crack propagation in materials. However, it is necessary to consider not only two-dimensional information obtained from micrographs of fracture surfaces but also three-dimensional morphology for more detailed analysis.

Various analyses associated with three-dimensional topography of fracture surfaces have been presented by using recently developed measurement instruments, for example, laser scanning microscope (LSM), atomic force microscope (AFM) and so on[1)-4)]. These instruments are characterized by high accuracy derived from direct measurement; however some difficulties arise especially in the case of the observation of rough surfaces at high magnification[5)].

On the other hand, the reconstruction of three-dimensional profiles of fracture surfaces from stereoscopic SEM micrographs has the advantage of suitability for very rough surfaces owing to its high depth of focus. Three-dimensional profiles reconstructed from digital images in a computer are generally called Digital Elevation Models (DEMs). The main problem for an automatic reconstruction of stereo image lies in finding corresponding points in two surface projections of a specimen, i.e., points in two stereo images have to be identified which are projections of the same object on the specimen.

Once a point is matched to the correspondent, the elevation of the point is calculated based on stereo-photogrammetric principle. In this method the accuracy of reconstructed DEMs significantly depends on the matching procedure; therefore a proper algorithm has to be introduced to the process[6)-10)].

In this study we develop an automatic reconstruction system for fractographic analysis which works on general personal computers and yields DEMs from stereoscopic SEM micrographs of investigated surfaces. Since SEM micrographs obtained from fracture surfaces of metals are ordinarily contrasty, the use of the area-based matching algorithm is considered to be valid for the searching procedure. At first a simple shaped object of known geometry is reconstructed by using the basic area-based method to verify the accuracy of the system. Next, a hierarchical

† Received on November 30, 2001
* Associate Professor
** Professor
*** Graduate student

Transactions of JWRI is published by Joining and Welding Research Institute of Osaka University, Ibaraki, Osaka 567-0047, Japan.

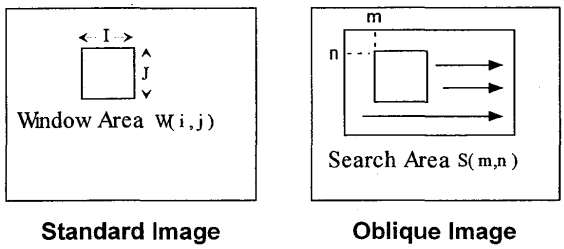

Fig. 1 Schematic illustration of the area-based matching algorithm.

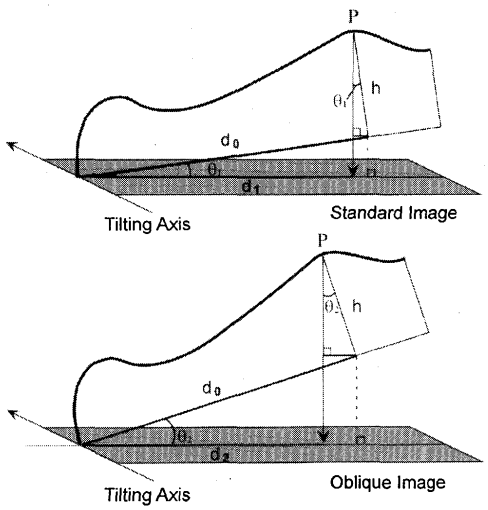

Fig. 2 Schematic illustration of stereo-photogrammetry.

technique is introduced to the algorithm, involving step-by-step decreasing of reference window size to improve the searching accuracy without the occurrence of matching failure.

The reconstruction procedure is applied to a ductile fracture surface of SUS329J3L duplex stainless steel, the topography of which is more complicated, and the validity of the reconstruction is evaluated in terms of quantitative fracture analysis.

2. Calculating Procedure

2.1 Process Flow of Three-dimensional Reconstruction

The stereo images are obtained from SEM images of tilted specimens in two different angles to each other. We adopted 4° and 8° as the tilt angle between the two images. The micrographs obtained were digitized by an image scanner with 256 gray levels. Subsequently, a pre-alignment procedure was conducted by translating and rotating images with respect to the specimen coordinates due to the inherent inaccuracy of an analog tilting stage and movements introduced during the digitizing. After that, the parallaxes between two images were measured by searching corresponding points using the area-based matching algorithm.

Figure 1 shows the schematic explanation of the area-based matching algorithm. A certain size of "window area" is placed on the first stereo image (called "standard image"). On the second stereo image ("oblique image") a window of the same dimension is moved around within a certain search area to find the position where the two windows show the maximum correspondence. A cross-correlation method was used for the estimation[11]. In Fig. 1 the cross-correlation coefficient of the two windows is calculated as follows:

$$R(m,n)=\frac{\sum_{j=0}^{J-1}\sum_{i=0}^{I-1}(W(i,j)-\overline{W})(S(m+i,n+j)-\overline{S}(m,n))}{\sqrt{\sum_{j=0}^{J-1}\sum_{i=0}^{I-1}(W(i,j)-\overline{W})^2}\sqrt{\sum_{j=0}^{J-1}\sum_{i=0}^{I-1}(S(m+i,n+j)-\overline{S}(m,n))^2}}$$
$$=\frac{\sum_{j=0}^{J-1}\sum_{i=0}^{I-1}(W(i,j)S(m+i,n+j))-IJ\overline{W}\,\overline{S}(m,n)}{\sqrt{\sum_{j=0}^{J-1}\sum_{i=0}^{I-1}(W(i,j)^2-IJ\overline{W}^2)}\sqrt{\sum_{j=0}^{J-1}\sum_{i=0}^{I-1}(S(m+i,n+j)^2-IJ\overline{S}(m,n)^2)}}, \quad (1)$$

where $W(i,j)$ and $S(m+i,n+j)$ are the gray levels of each pixel in the windows placed on the standard image and the oblique image respectively, and $\overline{W}$ and $\overline{S}(m,n)$ are average gray levels of each window which are represented by

$$\overline{W}=\frac{1}{IJ}\sum_{j=0}^{J-1}\sum_{i=0}^{I-1}W(i,j), \quad (2)$$

$$\overline{S}(m,n)=\frac{1}{IJ}\sum_{j=0}^{J-1}\sum_{i=0}^{I-1}S(m+i,n+j). \quad (3)$$

Then the centers of the two windows are chosen to be corresponding points. As shown in **Fig. 2**, the elevation of the matched point can be computed by the following equation:

$$h=\frac{d_1\cos\theta_2-d_2\cos\theta_1}{\sin(\theta_2-\theta_1)}, \quad (4)$$

where d_1 and d_2 are the distances from a standard point to the corresponding points and θ_1 and θ_2 are the tilt angles corresponding to the standard image and the oblique image respectively.

From the elevation data obtained, DEMs are displayed on a monitor via OpenGL; the library for two-dimensional and three-dimensional computer graphics programming. These programs were developed on "Microsoft Visual C++ 6.0" and designed to run under a Windows platform.

2.2. Quality of DEM Based on Image Discretization

The system has the minimum values with respect to surface geometry which are detectable from digital stereo images because of their discreteness. These values are determined numerically from the conditions of stereo-photogrammetry. For elevation, the minimum value is

identical with the elevation when parallax is equivalent to one pixel. It can be derived from Eq. (4) as

$$h_c = \frac{25.4}{M \cdot R|\sin\theta_1 - \sin\theta_2|}(mm), \qquad (5)$$

where h_c is the minimum value of detectable elevation and M and R are magnification and resolution of the image respectively. For lateral or vertical resolution, on the other hand, the minimum value is equivalent to the size of one pixel. However, DEMs mostly consist of discontinuous points extracted from several pixels, that is, the resolution of DEMs becomes greater than the minimum value and is represented by

$$d_c = \frac{25.4 \times I}{M \cdot R}(mm), \qquad (6)$$

where d_c is the lateral and vertical resolution of DEM and I is the interval value (pixel) of extraction. If the searching procedure is conducted properly, the errors in DEMs will lie within these values.

2.3. Verification of Surface Features on Known Geometry

To confirm the accuracy of this system it is necessary to perform a three-dimensional reconstruction of a simple object, the dimension of which is known. We chose Vickers hardness indent with pyramidal geometry for this purpose. **Figure 3** demonstrates a three-dimensional reconstruction of a Vickers hardness indent. The stereo pair was acquired at the magnification of 2250×, tilt angles of 0° and 4°, and the resolution of 300 dpi. By substituting these conditions in Eq. (5) the minimum value of detectable elevation of 0.54 μm is obtained. Though each facet of the indent is considered to be flat, there can be seen several steps associated with the minimum value in elevation in the reconstructed DEM. The diagonals were measured from the 0° image to evaluate the depth of the indent on the basis of the specified geometry of indentator. **Figure 4** shows the comparison between the obtained profile along the center of the indent and a theoretical profile calculated from the geometry of indentator. In Fig. 4 a good match can be seen between two profiles while the difference between the depths at the center is evaluated about 0.07 μm. Some discrepancies in the comparison may be due to spring-back in the material itself or out of the vertical in the central axis with respect to the material surface; that is the indent may not have the shape which was calculated on the basis of the specified geometry. From the fact that the difference of the maximum depth between two profiles lies within the minimum elevation value, accurate reconstruction can be expected in the case of simple objects.

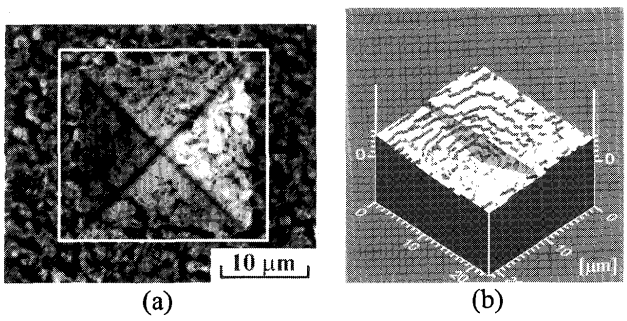

Fig. 3 Three-dimensional reconstruction of a Vickers hardness indent: (a) SEM micrograph, (b) Reconstructed DEM.

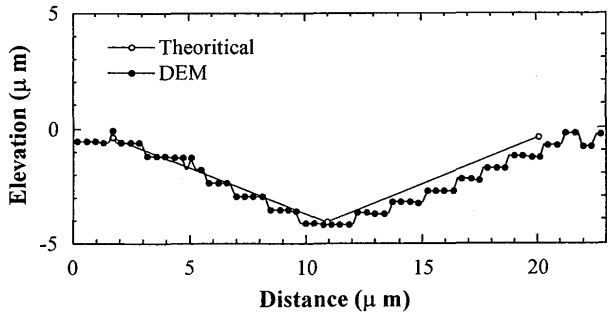

Fig. 4 Profile comparison of the Vickers hardness indent.

2.4. Applying Multi Step Searching Algorithm to Improve Searching Accuracy

On the other hand, reconstruction of objects which have relatively complicated shape such as ductile fracture surfaces requires high searching accuracy to acquire accurate DEMs. On the basis of an area-based matching algorithm, it can be considered that the size of window area has an influence on searching accuracy. It is desirable to make the window area as small as possible for accurate search[9]; however a small window size tends to cause matching errors (miss matching) attributed to the existence of similar areas in a search area.

In the previous work the window size has been determined experientially so that it satisfies both accuracy to some extent and robustness against miss matching[6)-8)]. Therefore, we have devised a multi step searching algorithm which intends to achieve high accuracy without occurrence of miss matching. The algorithm is hierarchical; at the first hierarchical level a pair of corresponding points are obtained with a sufficiently large window area and search area as the first estimation. Next, the size of the window area is reduced by 25% of the first one, and the search area is set so that its width is identical with that of the first window area and search is carried out around the first matched point. This procedure is repeated, and consequently accurate results can be obtained. This algorithm just aims to improve the searching accuracy in con-

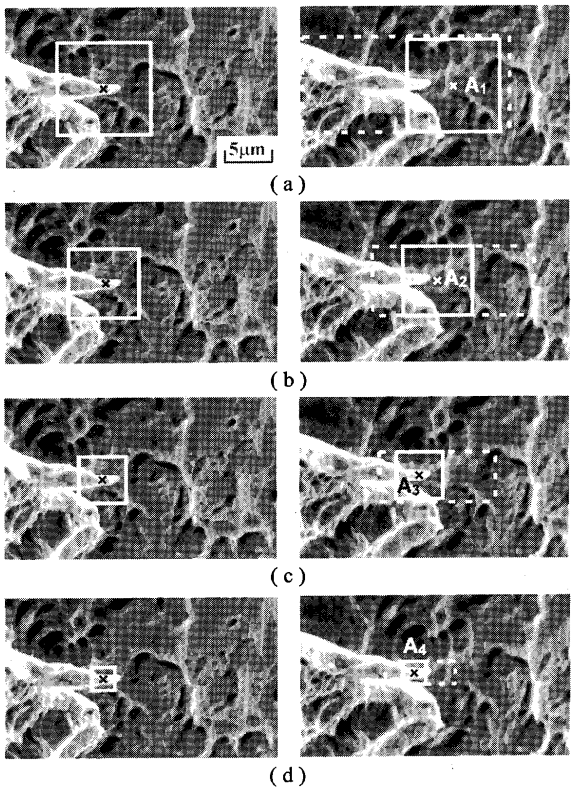

Fig. 5 Process of multi step searching applied to the fracture surface of SUS329J4L: (a) 1st step, (b) 2nd step, (c) 3rd step, (d) 4th step.

Table 1 Results of the multi step searching analysis.

Step of search	Coordinate of the corresponding point (pixel)	Deviation from the 4th step (pixel)	Elevation from the 4th step (μm)
1	A_1 (822,433)	209	-29.15
2	A_2 (739,432)	126	-17.57
3	A_3 (643,423)	30	-4.18
4	A_4 (613,422)	0	0

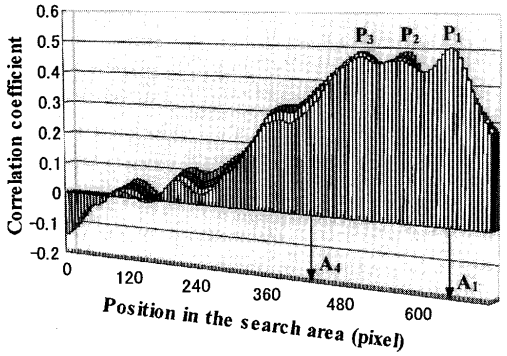

Fig. 6 The distribution map of the cross-correlation coefficient in the search area of the 1st searching step.

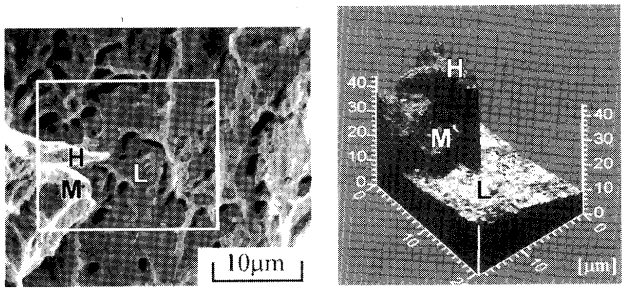

Fig. 7 Three-dimensional topography around the analysis point: (a) SEM micrograph, (b) DEM of the reconstructed fracture surface.

trast to the "course to fine" strategy for the reduction of computing time.

3. Results of Analysis

3.1. Accuracy of Multi Step Searching

Figure 5 shows a process of a multi step searching applied to a fracture surface obtained from a Charpy impact test of SUS329L4L duplex stainless steel. The left and right images are stereo pairs and the search is implemented in the right images to find the correspondents to the left. The four pairs of white squares of solid line represent corresponding areas at each step, the size of which are varied as 500×500→375×375→250×250→125×125 (pixel), and the x-marks are their centers. The rectangles of dotted line are the search areas at each step.

The analysis shows that the result is closing toward the correct point with the progression of the searching step, and at the final step it can be regarded to show almost correct matching. The details of the analysis are shown in **Table 1**. When regarding the 4th result (A_4) as a correct matching, there are differences in the elevation of 4.18 μm at the 3rd (A_3), 17.57 μm at the 2nd (A_2) and 29.15 μm at the 1st result (A_1) respectively.

Figure 6 shows the distribution map of cross-correlation coefficient in the search area at the 1st searching step. Several peaks can be seen around the site of the 1st result (A_1) and the peak corresponding to A_1 is a little higher than the peak near A_4 which is regarded as the site of correct matching.

Figure 7 shows (a) a SEM micrograph and (b) a DEM reconstructed by multi step searching around the analysis point. The reconstructed DEM reveals that three steps of different elevations, (they are marked as H, M, and L in the figure), exist around the analysis point. These steps are included in the window areas at each searching step, and parallaxes emerging in the respective regions vary depending on their elevations. Therefore, the matching result also varies according to which one is dominant in the window area. From this point, the position of the peaks of P_1 to P_3 in Fig. 6 can be related to the

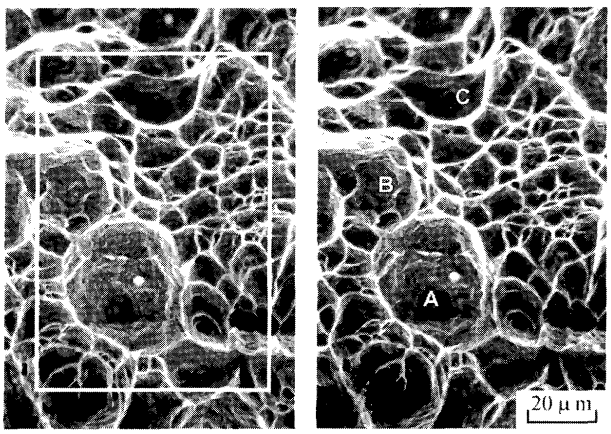

Fig. 8 Stereoscopic SEM micrographs of the fracture surface of SUS329J3L duplex stainless steel tested at 273K: (a) Standard image (0°), (b) Oblique image (8°).

parallaxes emerging in these three steps. At the first searching step, the L-region occupies the greater part of the window area, that makes the P_1 peak higher than other peaks. As the searching step progresses, the area fraction of the H-region in the window area increases and becomes dominant at the 4th step, which leads to correct matching.

3.2. Reconstructing DEM of Ductile Fracture Surface

The reconstruction procedure was applied to a fracture surface of a Charpy impact test for SUS329J3L duplex stainless steel. **Figure 8** shows stereoscopic SEM micrographs of the fracture surface. The testing temperature was 273K and dimple patterns can be observed in the micrographs. Two DEMs are presented in **Fig.9**. In Fig. 9(a) the DEM was reconstructed by single searching of the window area size of 120×120 (pixel), and in Fig. 9(b) multi step searching where the window area sizes were varied as 120×120→90×90→60×60 (pixel) was implemented to reconstruct the DEM. Both images exhibit highly indented surfaces with several steps. However, by applying multi step searching, Fig. 9(a) reveals the edge regions of dimple patterns more clearly, as well as the detailed features on the surface compared to Fig. 9(b).

In **Fig. 10(a)** and **Fig. 10(b)**, cross sectional profiles obtained from the DEMs in Fig. 9(a) and Fig. 9(b) respectively are shown. Both profiles were extracted from the same place of a dimple (marked as A); however different appearances can be seen especially in the shape of the edge of the dimple. Fig. 10(a) represents the typical dimple shape with keen edges, while dull edges are shown in Fig. 10(b). The difference of about 2.3 μm in depth can be observed between these two profiles. These results indicate that the use of the multi step searching algorithm suppresses the matching errors and represents

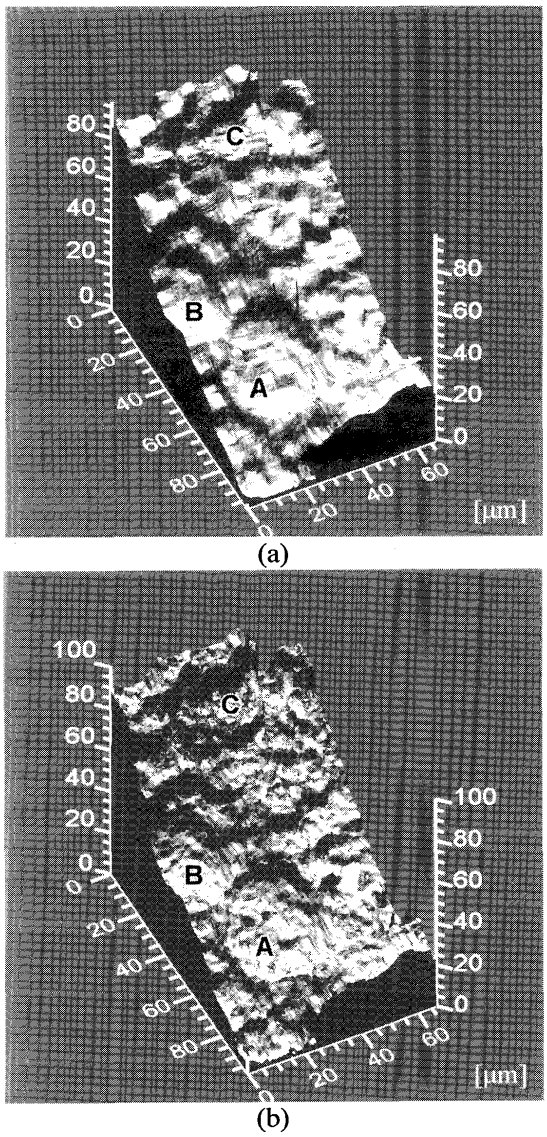

Fig. 9 DEMs of the fracture surface of SUS329J3L: (a) Reconstructed by single step searching, (b) Reconstructed by multi step searching.

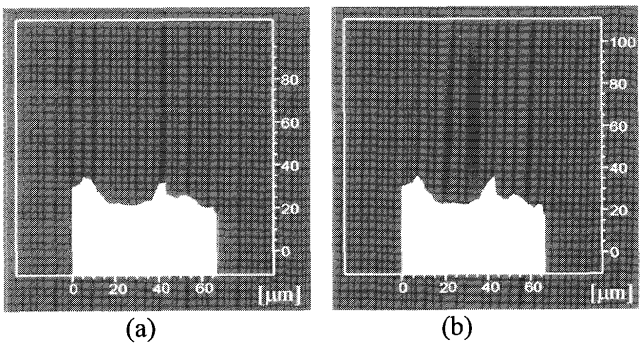

Fig. 10 Cross sectional profiles extracted from the same place of the dimple in the reconstructed DEMs: (a) Reconstructed by single step searching, (b) Reconstructed by multi step searching.

the real topography of the fracture surface.

4. Conclusions

In this study Digital Elevation Models (DEMs) of fracture surfaces were reconstructed from stereoscopic SEM micrographs using image processing techniques. The results obtained are summarized as follows.

(1) To verify the accuracy of the system a three-dimensional reconstruction of a Vickers hardness indent, the dimension of which is specified was performed. The analysis showed a good match between the obtained DEM and the theoretical profile of the indent.

(2) When a window area includes several regions of different elevations, the matching result depends on the area fraction of respective regions in the window area. A multi step searching algorithm devised in this work improved the searching accuracy of corresponding points in two stereo images.

(3) The multi step searching was applied to the ductile fracture surface of SUS329J3L duplex stainless steel. The reconstructed DEM clearly exhibits dimple shapes with tear ridges as well as detailed features on the fracture surface, which can be considered to provide useful information for quantitative fracture analysis.

References

1) T. Kobayashi, D. A. Shockey, C. G. Schmidt and R. W. Klopp, Int. J. Fatigue, 19 (1997) S237.
2) M. Fujiwara, K. Yoshimoto, and Y. Kondo, J. Soc. Mat. Sci., Japan, 46 (1997) 1107 (in Japanese).
3) M. Murata, Y. Mukai, Y. Taguchi and M. Hotta, Quar. J. Japan Welding Soc., 9 (1991) 453 (in Japanese).
4) S. Choi, H. Ishii and K. Tohgo, J. Soc. Mat. Sci., Japan, 47 (1998) 852 (in Japanese).
5) JSMS Committee on Fractography, Fractography, Maruzen, Tokyo (2000) (in Japanese).
6) K. Komai and J. Kikuchi, J. Soc. Mat. Sci., Japan, 34 (1984) 648 (in Japanese).
7) K. Komai and M. Noguchi, J. Iron and Steel Inst. Japan, 72 (1986) 2125 (in Japanese).
8) S. Sakai, H. Morita, H. Okamura and T. Takano, J. Japan Soc. Mech. Eng. A, 54 (1988) 2061 (in Japanese).
9) J. J. Ammann, L. R. Hein and A. M. Nazar, Mat. Characterization, 36 (1996) 379.
10) J. Stampfl, S. Sherer, M. Gruber and O. Kolednik, Appl. Phys. A, 63 (1996) 341.
11) J. A. Leese, C. S. Novak and B. B. Clark, J. Appl. Meteorol., 10 (1971) 118.